

Overpressure and its positive effect in deep sandstone reservoir quality of Bozhong
Depression, offshore Bohai Bay Basin, China

Xiao Wang^a, Sheng He^{a*}, Stuart Jones^b, Rui Yang^a, Ajuan Wei^c, Changhai Liu^d,
Qiang Liu^e, Chunyang Cheng^f, Weimin Liu^g

^a Key Laboratory of Tectonics and Petroleum Resources (Ministry of Education), China
University of Geosciences, Wuhan, China, 430074

^b Department of Earth Sciences, Durham University, Durham, UK, DH1 3LE

^c CNOOC Tianjin Co, Institution of Petroleum Exploration & Development, Tianjin, China,
300452

^d CNOOC EnerTech Drilling & Prod Co, Tianjin, China, 300452

^e PetroChina Jidong Oilfield Company, Tangshan, China, 063004

^f PetroChina Liaohe Oilfield Company, Panjin, China, 124005

^g SINOPEC Shengli Oilfield Company, Dongying, 257000, China

*Corresponding author, email address: shenghe@cug.edu.cn

1 **Abstract**

2 Bohai Bay Basin is a Meso-Cenozoic terrestrial sedimentary basin in eastern China. Its
3 offshore regions, including Bozhong and Liaodongwan Depressions, are favourable
4 exploration targets which provide near a half of the petroleum reserves in the basin. Eocene
5 Shahejie (Es) Formation and Oligocene Dongying (Ed) Formations are two important
6 exploration targets in Bozhong Depression, and overpressure is commonly seen in Es and Ed
7 Formations in this area. Our research examined the distribution characteristics of overpressure
8 in the formations and suggest the main mechanism of overpressure is compaction
9 disequilibrium due to the rapid sedimentation rates (~500m/Ma) of fine-grained sediments in
10 this area. Also, oil and gas generation within the thick mudstones of the two formations has
11 added the magnitude of overpressure. We investigated the reservoir quality especially primary
12 porosity in Es and Ed formations, and their relationship with overpressure. The positive effect
13 of overpressure on reservoir porosity preservation was validated through microscopic
14 observations and vertical effective stress (VES) analysis. We established a quantitative model
15 for evaluating the relationship of overpressure, pore structures, porosity, and VES. The result
16 suggests the overpressure in the targeted formations were primarily originated from
17 undercompaction. The overpressure kept VES from increasing and helped preserve the primary
18 intergranular porosity. The porosity preserved by overpressure can be significantly higher than
19 normally compacted porosity under the same condition of depth and temperature.

20

21 **Keywords:** overpressure; reservoir quality; Bohai Bay Basin; Shahejie Formation; Dongying
22 Formation

23

24 **1. Introduction**

25 Reservoir quality evaluation is vital in the exploration and development of deeper targets.
26 Pore geometry, porosity and permeability are the starting points of reservoir quality research
27 (Pittman, 1979; Ehrenberg, 1989, 1990). Deeply buried sandstones with anomalous porosity
28 and permeability are favourable reservoirs providing great probability for commercial
29 production. Anomalous porosity or permeability is statistically higher than the values in typical
30 sandstone reservoirs of a given lithology, age, and burial/temperature (Gluyas and Cade, 1997;
31 Bloch et al., 2002; Taylor et al., 2010). The controlling factors and mechanism of porosity
32 formation and preservation during diagenesis have long been investigated. Loucks et al. (1977)
33 studied the reservoir qualities of Lower Tertiary Frio Formation in Texas Gulf Coast and
34 proposed porosity in shallow reservoirs (<2500m) decrease due to compaction and cementation,
35 however, deeper reservoirs (2500~3500m) gain greater porosities from late subsurface leaching.
36 Bjørlykke (1992, 1998, and 2015) investigated clay mineral reactions in shales and sandstones
37 and discussed their importance in mechanical and chemical compactions. The characteristics
38 of clay coatings and their contribution to porosity preservation in deeply buried reservoirs have
39 also been studied worldwide (Pittman, 1992; Ehrenberg, 1993; Hammer et al., 2010; Morad et
40 al., 2010; Taylor et al., 2010; Maast et al., 2011; Dowey et al., 2012; Stricker et al., 2016a,
41 2018; Cui et al., 2017; Tang et al., 2018). Overpressure can make great impact on reservoir
42 quality as well. Scherer (1987) looked into thirteen parameters for their influence on primary
43 porosity in sandstones and suggested overpressure may resist the compaction process and
44 preserve primary porosity at a rate of 2% porosity for every 6.9 MPa (1,000 psi) overpressure.
45 Dixon et al. (1989) studied the preserved high primary porosity in deep Norphlet sandstones
46 (20% at depths of more than 6000 m) in Alabama and proposed migration of hydrocarbons and
47 geopressuring is one of the major factors of the preservation. Ramm et al. (1994) predicted the
48 porosity in Norwegian Continental Shelf and summarised the positive correlation between fluid
49 pressure and porosity. This positive correlation between porosity and overpressure has been
50 proved in the researches of the central North Sea (Kugler et al., 1990; Haszeldene et al., 1999;
51 Lander and Walderhaug, 1999; Osborne et al., 1999; Yardley et al., 2000; Lubanzadio et al.,
52 2002; Wilkinson et al., 2006; Goultly et al., 2012; Nguyen et al., 2013; Grant et al., 2014; Sathar
53 and Jones, 2016; Stricker et al., 2016b; Oye et al., 2018; O'neil et al., 2018).

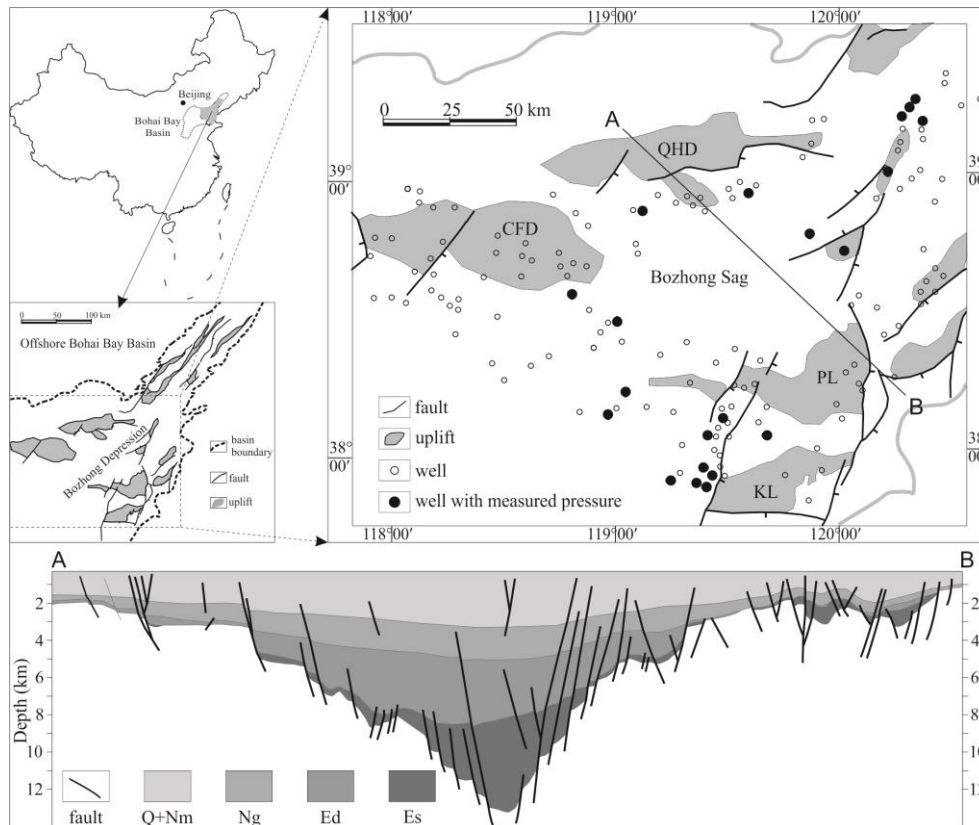
54 Pleistocene Dongying Formation (Ed) and Eocene Shahejie Formation (Es) are two deep
55 targets (>3000m) in the offshore regions of Bohai Bay Basin, in which overpressure is
56 commonly seen (Wang et al., 2016; Liu et al., 2016, 2017, 2019). In this work, the
57 characteristics of overpressure in Es and Ed are summarized, and the relationship between

58 overpressure and anomalous porosity is investigated through the comprehensive analysis of
59 wirelines, microscopic features, vertical effective stress, and test data including DST, core
60 porosity and permeability.

61 2. Geological settings

62 2.1 The structural settings

63 Bohai Bay Basin, also known as ‘Bohai Basin’ (Allen et al., 1997, 1998), is a “young”
64 sedimentary basin in eastern China. The recently published papers tend to reach an agreement
65 that Bohai Bay Basin is a rift basin reformed by strike-slip faulting (Cai et al., 2001; Hu et al.,
66 2001; Qi, 2004). The structural frame of the offshore regions, having the area of about 4.7×10^4
67 km² and currently covered by the Bohai Sea, is formed by Cenozoic tectonic deformation which
68 is a part of Himalayan tectonic movements (Mi and Duan, 2001; Xu et al., 2002; Xu et al.,
69 2006) and consists of two major depressions: Bozhong and Liaodongwan Depressions (Fig. 1).
70 Bozhong Depression is located in the south and in its centre formed the thickest sedimentation
71 (>11 km). Significant extension began in Bozhong Depression at approximately 43 ~ 45 Ma
72 ago. This syn-rift stage formed the thick layers of Es and Ed Formations and ceased at the end
73 of Oligocene. Then the post-rift thermal subsidence stage have been taking place since the
74 Miocene (24.6 Ma to present) (Cai et al., 2001; Qi, 2004; Gong, 2004; Zhou et al., 2010).



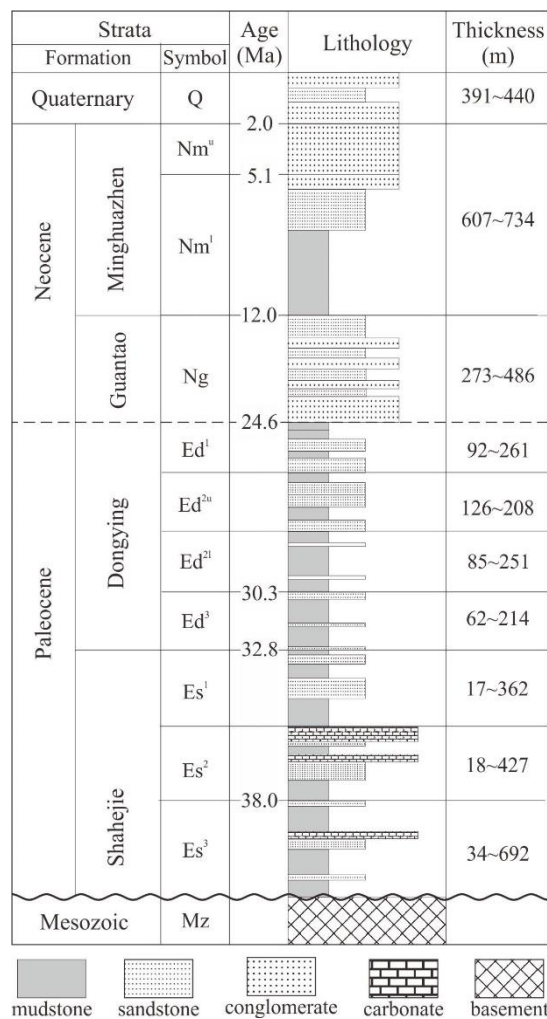
75

76

Figure 1. Location and structural distribution of Bozhong Depression.

77 **2.2 The stratigraphic settings**

78 The strata revealed by drilling in Bozhong Depression are (from bottom to top): Anz,
 79 Paleozoic (Pz), Mesozoic (Mz), Paleocene-Eocene Kongdian Formation (Ek), Eocene Shahejie
 80 Formation(Es), Oligocene Dongying Formation (generally accepted labelled as Ed), Lower-
 81 Neocene Guantao Formation (Ng), Upper-Neocene Minghuazhen Formation (Nm), and
 82 Quaternary (Qp) (Fig. 2). Their total thickness reached 12000m (39372 ft) in the Bozhong Sag
 83 which is the deepest sag of Bozhong Depression, among which Es and Ed Formations take up
 84 more than 70%. Es and Ed Formations are delta-lacustrine formations and form two main series
 85 of source rock and reservoirs.



86

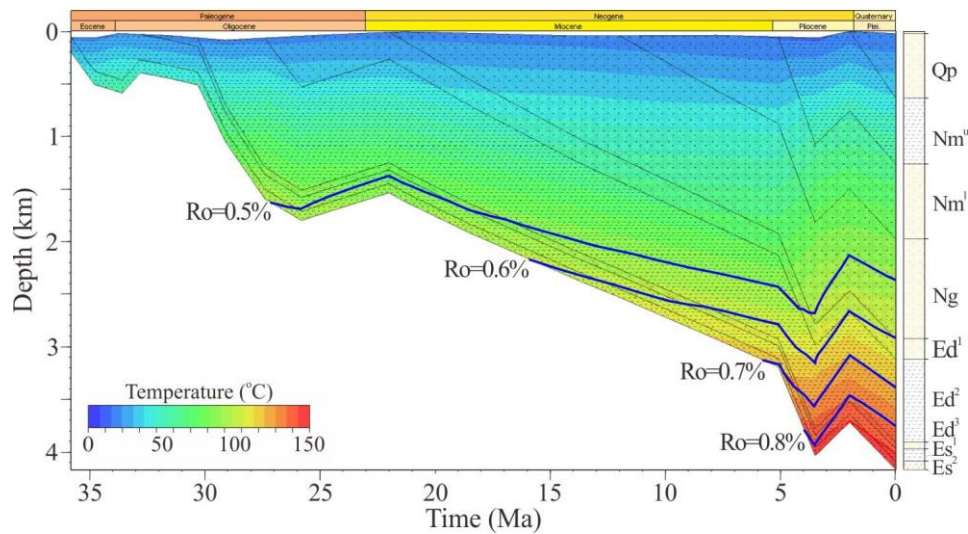
87

Figure 2. Summarized stratigraphic columns of offshore Bohai Bay Basin.

88 **2.3 The burial and thermal maturity history**

89 Es and Ed Formations are of great thickness in Bozhong Depression. Sedimentation rates
 90 of these two formations are relatively high, generally over 200m/Ma, highest reached 525m/Ma.
 91 The rapid sedimentation of Es and Ed made it difficult for pore pressure in and underneath
 92 Lower Ed to dissipate along the burial. This disequilibrium compaction directly caused the

93 over pressures in Es and Ed Formations. The estimation of pore pressure evolution shows the
 94 overpressure (pore pressure exceeds hydrostatic pressure) primarily emerged during the
 95 deposition of the second member of Ed Formation (Fig. 3).



96
 97

Figure 3. Burial and thermal history of Bozhong Depression.

98 3. Data and method

99 We used thin sections observations, core measurements, pore pressure data, and
 100 microscopic images to investigate the sandstone composition, reservoir property, pore pressure
 101 characteristics, and microscopic features corresponding to different pore pressure conditions.
 102 Basin modelling and VES analysis were used in analysing the origin and effect of overpressure.

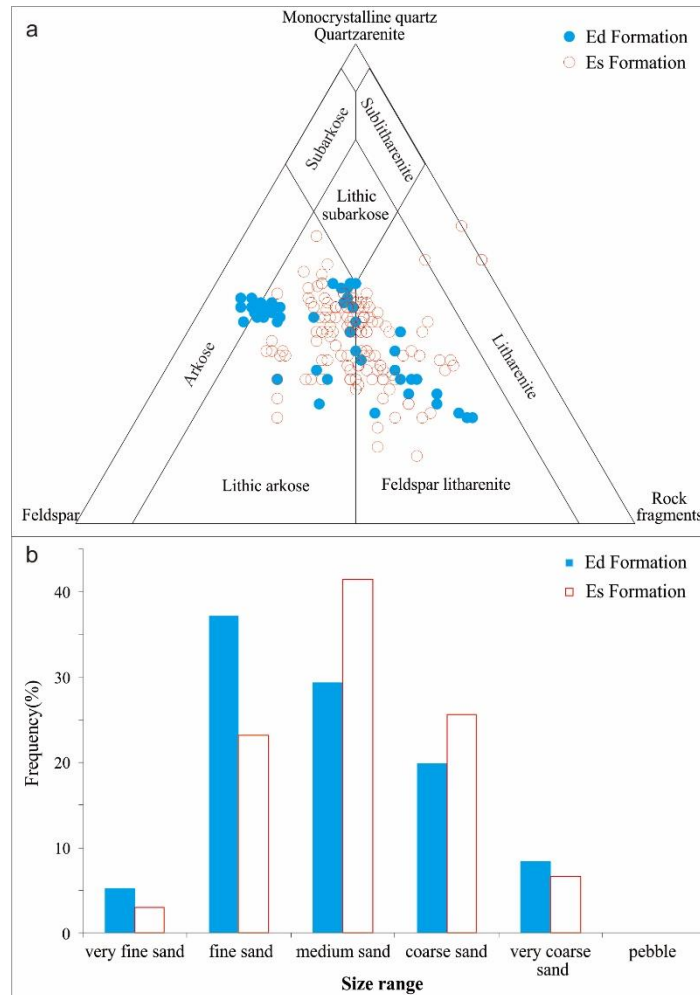
103 194 sandstone thin sections of Ed and Es Formations were observed. Grain size and
 104 sorting data were obtained by measuring the long axis of framework grains that were selected
 105 using a point count grid. 2376 sets of core measurements included porosity and Klinkenberg
 106 permeability at in situ stress and 270 DST pore pressure measurements were used in this study.
 107 89 Scanning electron microscopy (SEM) images were observed to examine the relationship
 108 between overpressure and microscopic textures.

109 4. Results

110 4.1 Sandstone composition and grain size

111 The Es Formation had been deposited through an environmental change of fluvial /delta
 112 – shallow/deep lacustrine – shallow lacustrine/ delta – lacustrine (Zhu et al., 2008). The
 113 changes formed four distinct members and sandstones are mainly encountered in the second
 114 and fourth members in Es Formation. Thin sections and casting thin section observations
 115 suggest the Es sandstones are mainly well sorted lithic arkose and Feldspar litharenite, and a
 116 small portion of arkose (Fig. 4a, red circles). The rock fragments are mainly from igneous and
 117 metamorphic rocks. The Ed Formation was dominantly formed in lacustrine environment with

118 delta sediments in the slopes. The Ed sandstones comprise lithic arkose and feldspar litharenite,
 119 in which lithic arkose takes up slightly more portions (Fig. 4a, blue filled circles). Es and Ed
 120 sandstones are generally fine-medium grained. The sandstones are coarser in Es Formation
 121 than which in Ed Formation (Fig. 4b).

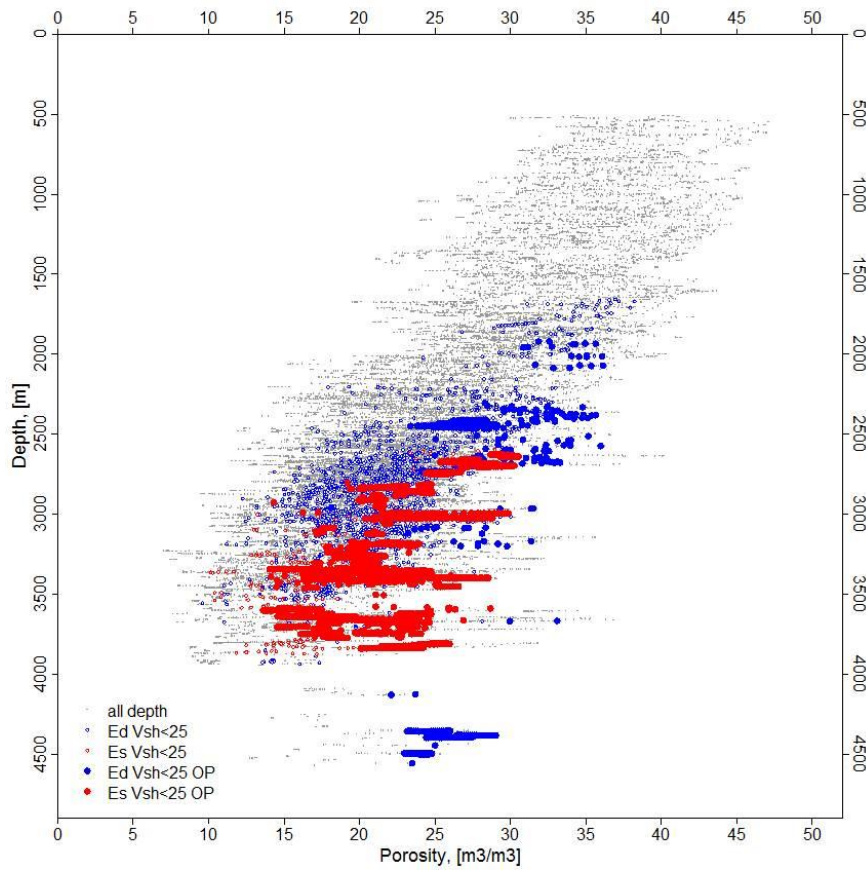


122 Figure 4. Composition and grain size of the Es and Ed sandstones in Bozhong Depression.

123 **4.2 Porosity and permeability**

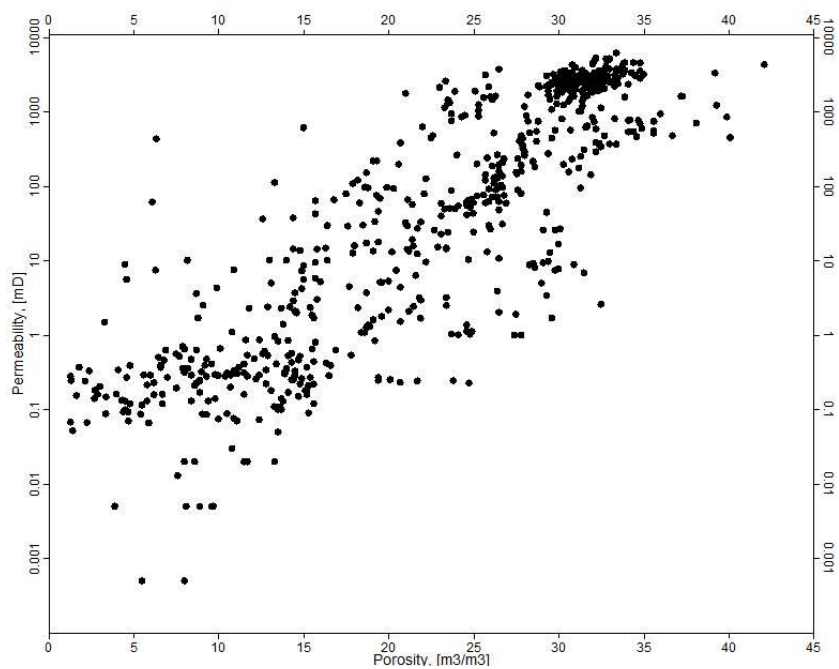
124 Core measured sandstone porosities in Es Formation range 10 ~ 30 % from the depth of
 125 2600 m; in Ed Formation they value 8~ 35% from the depth of 1700m (Fig. 5). The porosities
 126 in Es and Ed Formations generally demonstrate a decreasing trend versus depth, but off-trend
 127 high porosities are encountered in both formations. The porosity can reach 30% at the depth of
 128 ~4300 m (13124 ft.), which deviate from the regional porosity trend significantly. As the
 129 sandstone type and grain size don't vary substantially in the two formations, pore pressure is
 130 taken into account to explain the generation and maintaining of the off-trend high porosities in
 131 deep reservoir. Seen from the correlation of the porosities of the entire sandstone reservoir and
 132 porosities in the overpressured intervals, the off-trend high porosities predominantly fall in the
 133

134 overpressured intervals. Klinkenberg permeability in Bozhong Depression ranges 0.001 ~ 7000
135 mD and correlates well with porosities, suggesting the porosity can be relied solely to estimate
136 the reservoir quality (Fig. 6).



137
138

Figure 5. Porosity versus depth in Bozhong Depression.

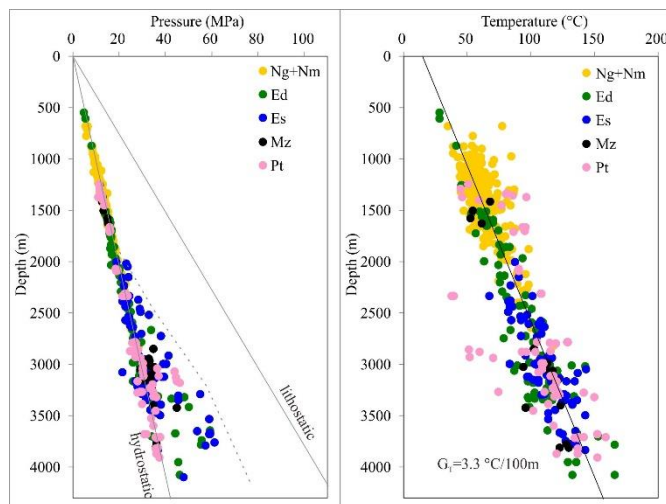


139
140

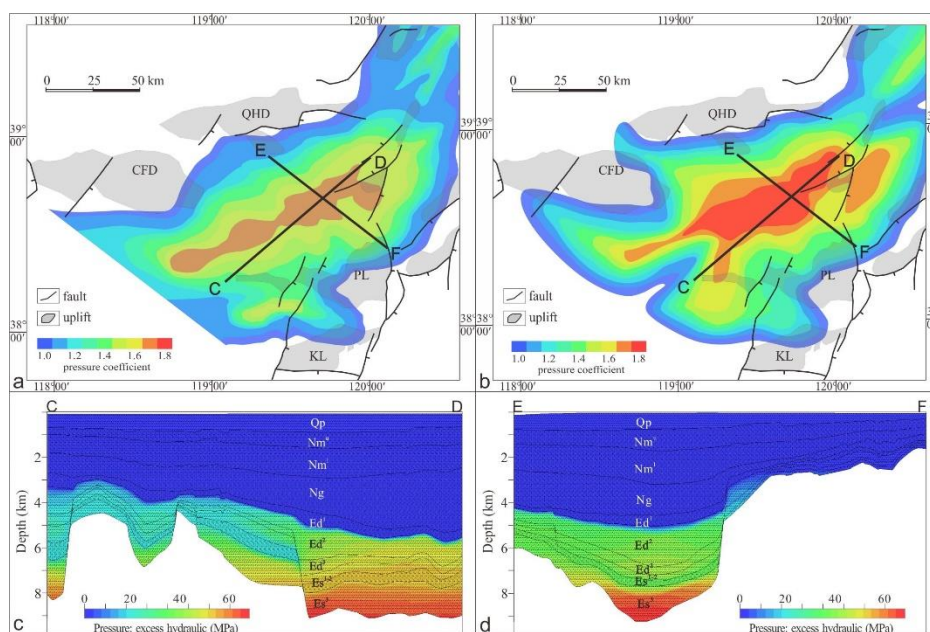
Figure 6. Porosity-permeability correlation in Bozhong Depression.

141 **4.3 Pore pressure characteristics in Bozhong Depression**

142 Vertically, DST data shows there are abnormally high pressures in Es and Ed Formations
 143 in this area (Fig. 7). Generally, the overpressure onset can be recognised from ~2500 m (8202
 144 ft.) in depth and get the greatest magnitude between 3500m and 3800m (11483~12467 ft.).
 145 Pore pressure in Ed Formation reaches 59.63 MPa (8647 psi) at the depth of 3650 m (11977
 146 ft.), with the overpressure coefficient (the ratio of pore pressure to hydrostatic pressure) of 1.65;
 147 in Es Formation, the maximum measured pore pressure, 61.46 MPa (8912 psi), occurs at the
 148 depth of 3768 m (12363 ft.). Wells revealed overpressure distribute around the Bozhong
 149 Depression (Fig. 8). There is no well drilled in the deep sag centre where current water depth
 150 of Bohai Sea reaches 85 m (279 ft.) or deeper, hence the regional distribution of overpressure
 151 was estimated from basin modelling.



152
 153 Figure 7. Measured data of pressure and temperature versus depth.



154
 155 Figure 8. Distribution maps and profiles of overpressure in Bozhong Depression.

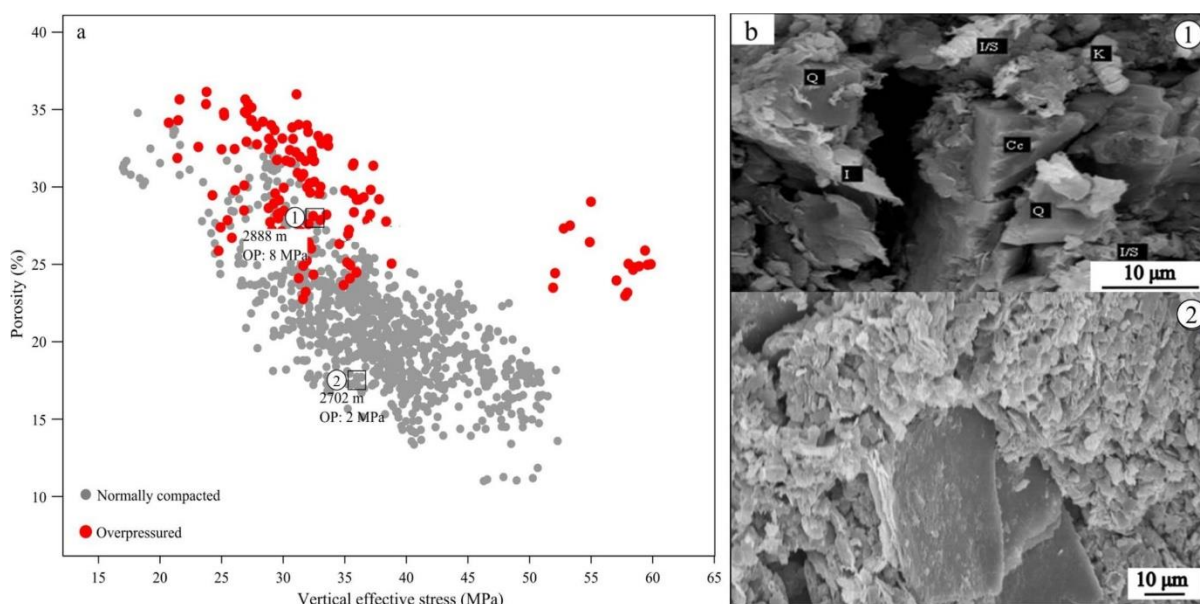
156

157 4.4 Microscopic characteristics

158 Micro analysis of porosity has been carried out to analysis the porosity preservation
159 situations in normally compacted sandstones and overpressured ones. SEM photos of the
160 sandstone samples are differentiated by their stratum and sedimentary facies. When compared,
161 the micro porosities of sandstones in same stratum and same facies show significant difference
162 as the pore pressure conditions are different

163 In Ed Formation, sample ① is taken from the depth of 2888 m (9475 ft.), the excess
164 hydrostatic pressure is 8MPa (1160 psi); Neutron porosity at this depth is ~27% (Fig. 9a). In
165 the SEM image, primary pores can be seen and the cementation is not severe. Cements are
166 quartz, illite, and some kaolinite (Fig. 9b, ①).

167 Sample ② is taken from the depth of 2702 m (8866 ft.), the excess hydrostatic pressure is
168 2 MPa (290 psi); Neutron porosity at this depth is ~17% (Fig. 9a). In the SEM image, primary
169 pores are filled by illite, kaolinite and some carbonate (Fig. 9b, ②).



170

171 Figure 9. The SEM images of Ed sandstones within different pore pressure horizons.

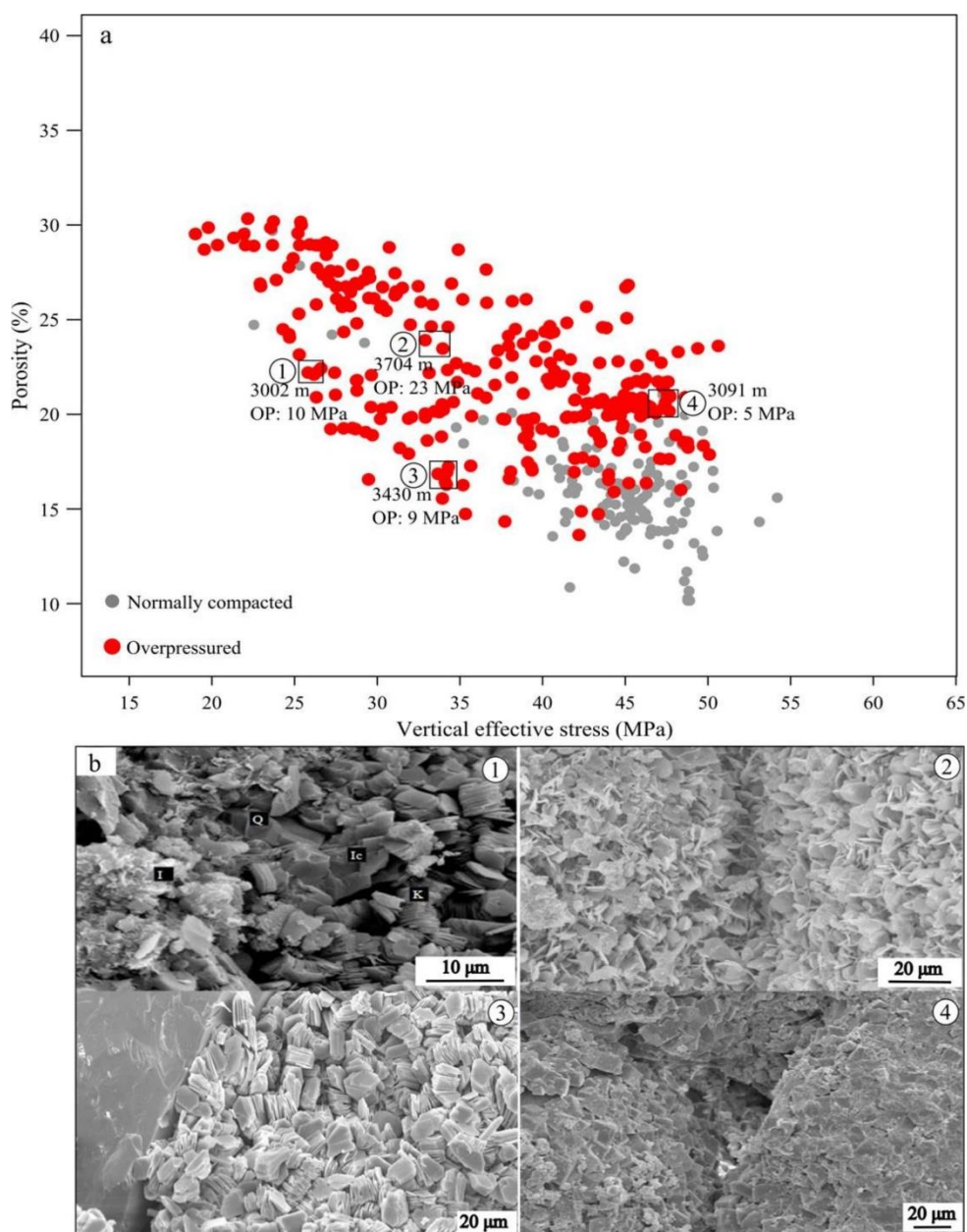
172 Unlike Ed Formation which is overpressured in deeper part, Es Formation is generally
173 overpressured. In Es Formation, sample ① is taken from the depth of 3002 m (9850 ft.), the
174 excess hydrostatic pressure is 10 MPa (1450 psi); Neutron porosity at this depth is ~23% (Fig.
175 10a). In the SEM image, primary pores can be seen and the cements are quartz, illite, and some
176 kaolinite (Fig. 10b, ①).

177 Sample ② is taken from the depth of 3704 m (12153 ft.), the excess hydrostatic pressure
178 is 23 MPa (3335 psi); Neutron porosity at this depth is ~24% (Fig. 10a). In the SEM image,

179 chlorite grain coats may help preserve the primary pores (Fig. 10b, ②). Though it is deeper,
180 the porosity maintains high compare to other samples.

181 Sample ③ is taken from the depth of 3430 m (11254 ft.), the excess hydrostatic pressure
182 is 9 MPa (1306 psi); Neutron porosity at this depth is ~17% (Fig. 10a). In the SEM image,
183 primary pores are filled by illite and kaolinite (Fig. 10b, ③). The overpressure magnitude is
184 relatively small considering its depth when compare to sample ①, and the porosity is smaller.

185 Sample ④ is taken from the depth of 3091 m (10141 ft.), the excess hydrostatic pressure is 5
186 MPa (725 psi); Neutron porosity at this depth is ~20% (Fig. 10a). In the SEM image, grains
187 are cemented by calcite and some kaolinite (Fig. 10b, ④).



188

189 Figure 10. The SEM images of Es sandstones within different pore pressure horizons.

190 **5. Discussion**

191 **5.1 The origin of overpressure**

192 As stated in the geological settings, Es and Ed Formations are of great thickness in
193 Bozhong Depression. Sedimentation rates of these two formations are relatively high, averaged
194 over 200 m/Ma, with the highest reached 525m/Ma (see section 2.3). In normal compaction
195 basin with similar age and lithology, the sedimentation rate is usually less than 100 m/Ma
196 (Ibach, 1982; Katz, 2005). The rapid sedimentation of Es and Ed prevented pore pressure in
197 and underneath Lower Ed to dissipate during the burial processes. This disequilibrium
198 compaction gradually accumulated overpressures in Es and Ed Formations. The estimation of
199 pore pressure evolution shows the overpressure (pore pressure exceeds hydrostatic pressure)
200 primarily emerged during the deposition of the middle member of Ed Formation (E_{3d}²) (see
201 Fig. 8).

202 Hydrocarbon generation is considered to be the second cause of overpressure. The source
203 rocks in Es and Ed Formations were buried deep during the rapid burial which may have
204 accelerated their maturation and generation behaviour. Source rocks in Es and Ed Formations
205 have a vitrinite reflectance (R_o) values of 0.6% or higher under the depth of 2500 m (8203 ft.).

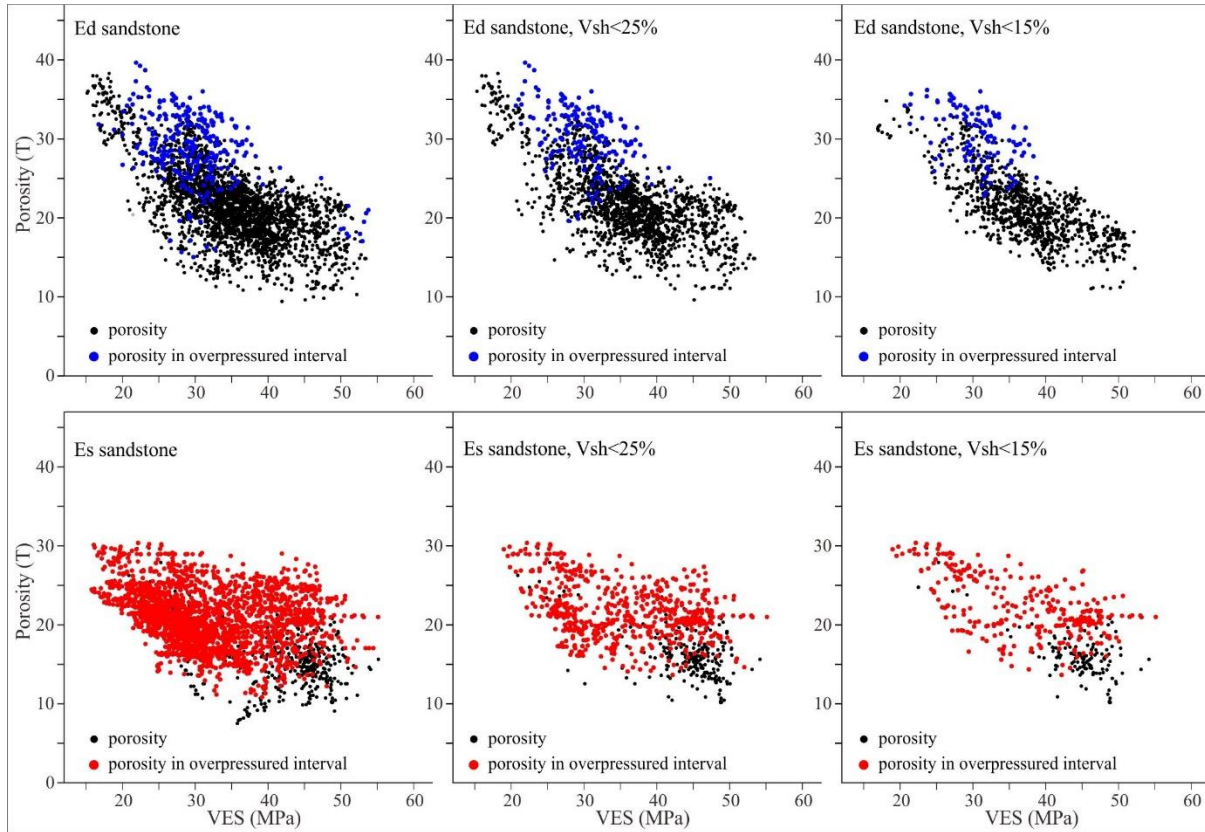
206 **5.2 Vertical effective stress – porosity relationships**

207 Since the overpressure in Bozhong Depression is mainly caused by disequilibrium
208 compaction, mechanical compaction may have controlled the primary porosity preservation in
209 sandstones. We used equation derived from Terzaghi's effective stress principle to investigate
210 the VES (Nur and Byerlee, 1971; Tuncay and Corapcioglu, 1995). The relationship of porosity
211 and vertical effective stress (VES) is employed in this research to investigate the process of
212 mechanical compaction and its effect on the porosities. Sandstone porosities in Es and Ed
213 Formations generally show a decreasing trend while the VES increases (Fig. 11, first column).
214 The porosities in overpressured horizons are on the trend but a bit higher at same VES
215 compared to which in normal pressured horizons, which may indicate overpressured
216 sandstones have better porosity than normally compacted ones at the same depth.

217 The compaction rate of sandstones varies significantly from facies to facies. The finer
218 grained sediments can be compacted relatively faster and easier than coarse grains. To
219 eliminate the facies variation effect in compaction process, shale content (V_{sh}) is introduced
220 to investigate the VES – porosity relationship in similar sandstones. Considering the facies
221 evolution in Bozhong Depression, sandstones have V_{sh} less than 25% formed in shallow
222 lacustrine or slope, V_{sh} less than 15% mostly occur in delta front. As in Fig. 11 (middle and
223 right columns), sandstones with V_{sh} less than 15% show the most distinct and uniform

224 decreasing trend. The high pore pressure horizons, which are the low in VES, correlate to high
225 porosities. This indicates overpressure helped preserving the primary porosity.

226 Some anomalously high porosity occurs in Ed Formation in a deep well (stays 25~30 %
227 below 4300 m / Fig. 11, upper row). This porosity may be added by the secondary dissolution
228 porosity.

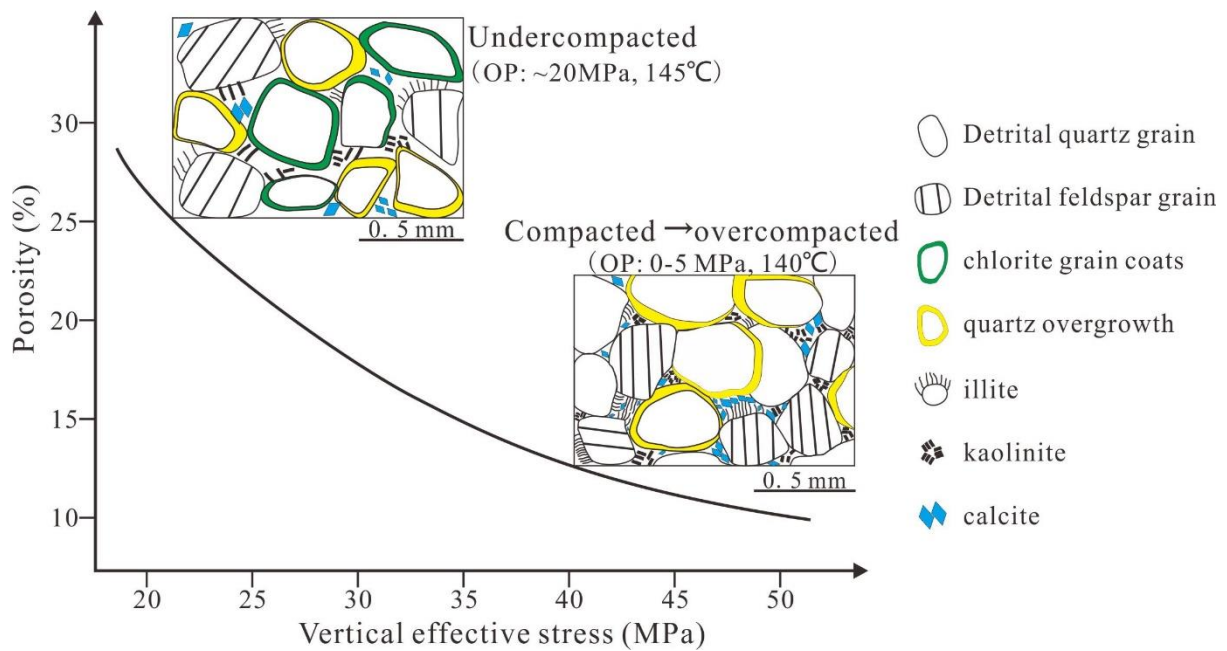


229
230 Figure 11. The relationship of porosity and vertical effective stress in Bozhong Depression.

231 5.3 Schematic model of the preservation effect of overpressure on sandstone porosity

232 Based on the above analysis, we have established a schematic model which illustrate the
233 vertical effective stress and sandstone porosity evolution (Fig. 12). The intention of this model
234 is to provide a quantitative reference for the relationship of overpressure, pore structures,
235 porosity, and VES. For normally compacted sandstone reservoirs which consists mainly of
236 quartz and feldspars and have initial primary intergranular porosity of ~30%, the initial VES
237 would be ~20 MPa. The contact of grains were point contact, and cementation was weak. With
238 the burial depth increasing, the VES increased. With increasing VES, the contact of matrix
239 grains in sandstones became tighter, from point contact to line contact. The primary
240 intergranular pores became smaller or even vanished. When VES reached ~40 MPa, the
241 primary intergranular porosity would decline to less than 15%. However, the primary
242 intergranular porosity in undercompacted reservoir (having an overpressure magnitude of ~20

243 MPa) can retain 25% at the similar depth. Undercompaction induced overpressures would be
 244 preserved in the matrix unless deformed afterwards, hence they can resist the stress act upon
 245 sandstone grains, keeping the VES from increasing. Therefore, the compaction between matrix
 246 grains and reservoir porosity were protected by overpressure. The primary intergranular
 247 porosity preserved by overpressure can be more than 10% higher than normally compacted
 248 porosity under the same condition of depth and temperature.



249
 250 Figure 12. The schematic diagram of the relationship between VES and porosity.

251 **6. Conclusion**

252 Extensive overpressure has been encountered in Bozhong Depression of offshore Bohai
 253 Bay Basin. The overpressure is mainly confined in the Es and Ed Formations, and the pore
 254 pressure can reach ~60 MPa (8700 psi) at the depth of ~3700 m (12140 ft.) according to the
 255 measured data. Disequilibrium compaction is identified as the main mechanism of overpressure
 256 generation in this area. Hydrocarbon generation has added to the amount of overpressure at the
 257 present day.

258 Reservoir quality of sandstone in the Es and Ed Formations is variable but there are off-
 259 trend high porosities which can be up to 30% at the depth of ~4000 m (13124 ft.). Almost all
 260 of these off-trend high porosities are recorded in the intervals with overpressure. Porosity-
 261 vertical effective stress analysis and the micro pore structures validate the positive effect of
 262 overpressure on high porosity preservation. The primary intergranular porosity preserved by
 263 overpressure can be more than 10% higher than normally compacted porosity under the same
 264 condition of depth and temperature.

265

266 **Acknowledgments**

267 This work was supported by the Fundamental Research Funds for the Central Universities, China
268 University of Geosciences (Wuhan), and China National Science and Technology Major Project (No.
269 2016ZX05006-003-001). Xiao Wang's visiting study in Durham University was supported by China
270 Scholarship Council (No. 201406410047).

271 **References**

- 272 Allen, M., Macdonald, D., Xun, Z., Vincent, S., and Brouet-Menzies, C., 1997. Early
273 Cenozoic two-phase extension and late Cenozoic thermal subsidence and inversion of
274 the Bohai Basin, northern China. *Marine and Petroleum Geology*, 14: 951-972.
275 [http://dx.doi.org/10.1016/S0264-8172\(97\)00027-5](http://dx.doi.org/10.1016/S0264-8172(97)00027-5)
- 276 Allen, M. B., Macdonald, D. I., Xun, Z., Vincent, S. J., and Brouet-Menzies, C., 1998.
277 Transtensional deformation in the evolution of the Bohai Basin, northern China.
278 *Geological Society, London, Special Publications*, 135: 215-229.
279 <http://dx.doi.org/10.1144/GSL.SP.1998.135.01.14>
- 280 Bjørlykke, K., and Aagaard, P., 1992. Clay minerals in North Sea sandstones, in
281 Houseknecht, D. W. and Pittman, E. D. eds., *Origin, diagenesis, and petrophysics of*
282 *clay minerals in sandstones*. Tulsa, Oklahoma, SEPM: 65-80.
- 283 Bjørlykke, K., 1998. Clay mineral diagenesis in sedimentary basins-a key to the prediction of
284 rock properties. Examples from the North Sea Basin. *Clay Minerals*, 33: 15-34.
285 <http://dx.doi.org/10.1180/claymin.1998.033.1.03>
- 286 Bjørlykke, K., and Jahren, J., 2015. *Sandstones and sandstone reservoirs*, Petroleum
287 Geoscience. Springer.
- 288 Bloch, S., Lander, R. H., and Bonnell, L. M., 2002. Anomalously high porosity and
289 permeability in deeply buried sandstone reservoirs: Origin and predictability. *AAPG*
290 *Bulletin*, 86: 301-328. [http://dx.doi.org/10.1306/61eedabc-173e-11d7-](http://dx.doi.org/10.1306/61eedabc-173e-11d7-8645000102c1865d)
291 [8645000102c1865d](http://dx.doi.org/10.1306/61eedabc-173e-11d7-8645000102c1865d)
- 292 Cai, D., Yuhui, L., Wenlai, W., and Changhua, Y., 2001. Shallow tectonic deformation and
293 its relationship to hydrocarbon enrichment in Bozhong Depression and adjacent areas,
294 Bohai Bay Basin. *China Offshore Oil and Gas*, 1: 006-010.
- 295 Cui, Y., Jones, S. J., Saville, C., Stricker, S., Wang, G., Tang, L. and Chen, J., 2017. The role
296 played by carbonate cementation in controlling reservoir quality of the Triassic
297 Skagerrak Formation, Norway. *Marine and Petroleum Geology*, 85: 316-331.
298 <http://dx.doi.org/10.1016/j.marpetgeo.2017.05.020>

299 Dixon, S. A., Summers, D. M., and Surdam, R. C., 1989. Diagenesis and preservation of
300 porosity in Norphlet Formation (Upper Jurassic), southern Alabama. AAPG Bulletin,
301 73: 707-728.

302 Dowey, P. J., Hodgson D. M., and Worden, R. H., 2012. Prerequisites, processes, and
303 prediction of chlorite grain coatings in petroleum reservoirs: A review of subsurface
304 examples. *Marine and Petroleum Geology*, 32: 63-75.
305 <http://dx.doi.org/10.1016/j.marpetgeo.2011.11.007>

306 Ehrenberg, S., 1989. Assessing the relative importance of compaction processes and
307 cementation to reduction of porosity in sandstones: Discussion. AAPG Bulletin, 73:
308 1274-1276. <http://dx.doi.org/10.1306/44B4AA1E-170A-11D7-8645000102C1865D>

309 Ehrenberg, S., 1990. Relationship between diagenesis and reservoir quality in sandstones of
310 the Garn formation, Haltenbanken, mid-Norwegian Continental shelf. AAPG Bulletin,
311 74: 1538-1558.

312 Ehrenberg, S., 1993. Preservation of anomalously high porosity in deeply buried sandstones
313 by grain-coating chlorite: examples from the Norwegian continental shelf. AAPG
314 Bulletin, 77: 1260-1286. [http://dx.doi.org/10.1306/BDF8E5C-1718-11D7-
315 8645000102C1865D](http://dx.doi.org/10.1306/BDF8E5C-1718-11D7-8645000102C1865D)

316 Gluyas, J. G., and Cade, C. A., 1997. Prediction of porosity in compacted sands, in J. A.
317 Kupecz, J. G. Gluyas, and C. A. Cade, eds., *Reservoir quality prediction in sandstones
318 and carbonates*. AAPG Memoir, 69: 19-28.

319 Gong, Z., 2004. Neotectonic movement and hydrocarbon accumulation in petroliferous
320 basins, offshore China. *Oil & Gas Geology*, 2:562-570. (in Chinese)

321 Goultly, N., Ramdhan, A., and Jones, S., 2012. Chemical compaction of mudrocks in the
322 presence of overpressure. *Petroleum Geoscience*, 18: 471-479.
323 <http://dx.doi.org/10.1144/petgeo2012-018>

324 Grant, N. T., Middleton, A. J., and Archer, S., 2014. Porosity trends in the Skagerrak
325 Formation, Central Graben, United Kingdom Continental Shelf: The role of compaction
326 and pore pressure history. AAPG Bulletin, 98: 1111-1143.
327 <http://dx.doi.org/10.1306/10211313002>

328 Hammer, E., Mork, M. B. E., and Naess, A., 2010. Facies controls on the distribution of
329 diagenesis and compaction in fluvial-deltaic deposits. *Marine and Petroleum Geology*,
330 27: 1737-1751. <http://dx.doi.org/10.1016/j.marpetgeo.2009.11.002>

331 Haszeldene, R. S., Wilkinson, M., Darby, D., Macaulay, C. I., Couples, G. D., Fallick, A. E.,
332 Fleming, C. G., Stewart, R. N. T., and McAulay, G., 1999. Diagenetic porosity creation

333 in an overpressured graben, in Fleet, A. J. and Boldy, S. A. eds., Petroleum geology of
334 northwest Europe. Proceedings of the 5th Conference: London, United Kingdom,
335 Geological Society.

336 Hu, S., O'Sullivan, P. B., Raza, A., and Kohn, B. P., 2001. Thermal history and tectonic
337 subsidence of the Bohai Basin, northern China: a Cenozoic rifted and local pull-apart
338 basin. *Physics of the Earth and Planetary Interiors*, 126: 221-235.
339 [http://dx.doi.org/10.1016/S0031-9201\(01\)00257-6](http://dx.doi.org/10.1016/S0031-9201(01)00257-6)

340 Ibach, L. E. J., 1982. Relationship between sedimentation rate and total organic carbon
341 content in ancient marine sediments. *AAPG Bulletin*, 66(2): 170-188.

342 Katz, B. J., 2005. Controlling factors on source rock development-a review of productivity,
343 preservation, and sedimentation rate. *SEPM Special Publication*, 82:7-16.
344 <http://dx.doi.org/10.2110/pec.05.82.0007>

345 Kugler, R. L., and McHugh, A., 1990. Regional diagenetic variation in Norphlet Sandstone:
346 Implications for reservoir quality and the origin of porosity. *Gulf Coast Association of*
347 *Geological Societies Transactions*, 40: 411-423.

348 Lander, R.H., and Walderhaug, O., 1999. Predicting porosity through simulating sandstone
349 compaction and quartz cementation. *AAPG Bulletin*, 83: 433-449.

350 Liu, H., Jiang, Y., Song, G., Gu, G., Hao, L., and Feng, Y., 2017. Overpressure
351 characteristics and effects on hydrocarbon distribution in the Bonan Sag, Bohai Bay
352 Basin, China. *Journal of Petroleum Science and Engineering*, 149: 811-821.
353 <http://dx.doi.org/10.1016/j.petrol.2016.11.029>

354 Liu, H., Jing, C., Jiang, Y., Song, G., Yu, Q., and Feng, Y., 2016. Characteristics and genetic
355 mechanisms of overpressure in the depressions of Bohai Bay Basin, China. *Acta*
356 *Geologica Sinica - English Edition*, 906: 2216-2228. [http://dx.doi.org/10.1111/1755-](http://dx.doi.org/10.1111/1755-6724.13032)
357 [6724.13032](http://dx.doi.org/10.1111/1755-6724.13032)

358 Liu, H., Yuan, F., Jiang, Y., Zhao, M., Chen, K., Guo, Z., and Wang, Y., 2019. Mechanisms
359 for overpressure generated by the undercompaction of paleogene strata in the Baxian
360 Depression of Bohai Bay Basin, China. *Marine and Petroleum Geology*, 99: 337-346.
361 <http://dx.doi.org/10.1016/j.marpetgeo.2018.10.001>

362 Loucks, R., Bebout, D., and Galloway, W. E., 1977. Relationship of Porosity Formation and
363 Preservation to Sandstone Consolidation History--Gulf Coast Lower Tertiary Frio
364 Formation. *Gulf Coast Association of Geological Societies Transactions*, 27:109-120.

365 Lubanzadio, M., Goult, N. R., and Swarbrick, R. E., 2002. Variation of velocity with
366 effective stress in chalk: Null result from North Sea well data. *Marine and Petroleum*
367 *Geology*, 19: 921-927. [http://dx.doi.org/10.1016/S0264-8172\(02\)00135-6](http://dx.doi.org/10.1016/S0264-8172(02)00135-6)

368 Maast, T. E., Jahren, J., and Bjørlykke, K., 2011. Diagenetic controls on reservoir quality in
369 Middle to Upper Jurassic sandstones in the South Viking Graben, North Sea. *AAPG*
370 *Bulletin*, 95:1937-1958. <http://dx.doi.org/10.1306/03071110122>

371 Mi, L., and Duan, J., 2001. Characteristics of middle and shallow strata oil-gas reservoirs and
372 oil-gas accumulation rule in the middle area of Bohai. *Acta Petrolei Sinica*, 2: 006-010.
373 (in Chinese)

374 Morad, S., Al-Ramadan, K., Ketzer, J. M., and De Ros, L. F., 2010. The impact of diagenesis
375 on the heterogeneity of sandstone reservoirs: A review of the role of depositional facies
376 and sequence stratigraphy. *AAPG Bulletin*, 94: 1267-1309.
377 <http://dx.doi.org/10.1306/04211009178>

378 Nguyen, B. T., Jones, S. J., Goult, N. R., Middleton, A. J., Grant, N., Ferguson, A., and
379 Bowen, L., 2013. The role of fluid pressure and diagenetic cements for porosity
380 preservation in Triassic fluvial reservoirs of the Central Graben, North Sea. *AAPG*
381 *Bulletin*, 97: 1273-1302. <http://dx.doi.org/10.1306/01151311163>

382 Nur, A., and Byerlee, J., 1971. An exact effective stress law for elastic deformation of rock
383 with fluids. *Journal of Geophysical Research*, 76(26): 6414-6419.
384 <http://dx.doi.org/10.1029/JB076i026p06414>

385 O'Neill, S. R., Jones, S. J., Kamp, P. J., Swarbrick, R. E., and Gluyas, J. G., 2018. Pore
386 pressure and reservoir quality evolution in the deep Taranaki Basin, New Zealand.
387 *Marine and Petroleum Geology*, 98: 815-835.
388 <http://dx.doi.org/10.1016/j.marpetgeo.2018.08.038>

389 Osborne, M. J., and Swarbrick, R. E., 1999. Diagenesis in North Sea HPHT clastic reservoirs:
390 Consequences for porosity and overpressure prediction. *Marine and Petroleum Geology*,
391 16: 337-353. [http://dx.doi.org/10.1016/s0264-8172\(98\)00043-9](http://dx.doi.org/10.1016/s0264-8172(98)00043-9)

392 Oye, O. J., Aplin, A. C., Jones, S. J., Gluyas, J. G., Bowen, L., Orland, I. J., and Valley, J.
393 W., 2018. Vertical effective stress as a control on quartz cementation in sandstones.
394 *Marine and Petroleum Geology*, 98: 640-652.
395 <http://dx.doi.org/10.1016/j.marpetgeo.2018.09.017>

396 Pittman, E. D., 1979. Porosity diagenesis and productive capability of sandstone reservoirs.
397 *SEPM Special Publication*, 26: 157-173. <http://dx.doi.org/10.1306/C1EA4545-16C9-11D7-8645000102C1865D>

398

399 Pittman, E. D., Larese R. E., and Heald, M. T., 1992. Clay coats: Occurrence and relevance to
400 preservation of porosity in sandstones. *SEPM Special Publication*, 47: 241-255.
401 <http://dx.doi.org/10.2110/pec.92.47.0241>

402 Qi, J., 2004. Two tectonic systems in the Cenozoic Bohai Bay basin and their genetic
403 interpretation. *Chinese Geology*, 1: 001-005. (in Chinese)

404 Ramm, M., and Bjørlykke, K., 1994. Porosity/depth trends in reservoir sandstones:
405 Assessing the quantitative effects of varying pore-pressure, temperature history and
406 mineralogy, Norwegian Shelf data. *Clay Minerals*, 29: 475-490.
407 <http://dx.doi.org/10.1180/claymin.1994.029.4.07>

408 Sathar, S., and Jones, S., 2016. Fluid overpressure as a control on sandstone reservoir quality
409 in a mechanical compaction dominated setting: Magnolia Field, Gulf of Mexico. *Terra*
410 *Nova*, 283: 155-162. <http://dx.doi.org/10.1111/ter.12203>

411 Scherer, M., 1987. Parameters influencing porosity in sandstones: a model for sandstone
412 porosity prediction. *AAPG Bulletin*, 71: 485-491. [http://dx.doi.org/10.1306/703C80FB-
413 1707-11D7-8645000102C1865D](http://dx.doi.org/10.1306/703C80FB-1707-11D7-8645000102C1865D)

414 Stricker, S., Jones, S. J., and Grant, N. T. 2016b. Importance of vertical effective stress for
415 reservoir quality in the Skagerrak Formation, Central Graben, North Sea. *Marine and*
416 *Petroleum Geology*, 78: 895-909. <http://dx.doi.org/10.1016/j.marpetgeo.2016.03.001>

417 Stricker, S., Jones, S. J., Meadows, N., and Bowen, L., 2018. Reservoir quality of fluvial
418 sandstone reservoirs in salt-walled mini-basins: an example from the Seagull field,
419 Central Graben, North Sea, UK. *Petroleum Science*, 151: 1-27.
420 <http://dx.doi.org/10.1007/s12182-017-0206-x>

421 Stricker, S., Jones, S. J., Sathar, S., Bowen, L., and Oxtoby, N., 2016a. Exceptional reservoir
422 quality in HPHT reservoir settings: examples from the Skagerrak Formation of the
423 Heron Cluster, North Sea, UK. *Marine and Petroleum Geology*, 77: 198-215.
424 <http://dx.doi.org/10.1016/j.marpetgeo.2016.02.003>

425 Tang, L. X., Gluyas, J., Jones, S., and Bowen, L., 2018. Diagenetic and geochemical studies
426 of the Buchan Formation Upper Devonian in the Central North Sea. *Petroleum Science*,
427 152: 211-229. <http://dx.doi.org/10.1007/s12182-018-0232-3>

428 Taylor, T. R., Giles, M. R., Hathon, L. A., Diggs, T. N., Braunsdorf, N. R., Birbiglia, G. V.,
429 Kittridge, M. G., Macaulay, C. I., and Espejo, I. S., 2010. Sandstone diagenesis and
430 reservoir quality prediction: Models, myths, and reality. *AAPG Bulletin*, 94: 1093-1132.
431 <http://dx.doi.org/10.1306/04211009123>

- 432 Tuncay, K., and Corapcioglu, M. Y., 1995. Effective stress principle for saturated fractured
433 porous media. *Water Resources Research*, 31(12): 3103-3106.
434 <http://dx.doi.org/10.1029/95WR02764>
- 435 Wang, X., He, S., Wei, A., Liu, Q., and Liu, C., 2016. Typical disequilibrium compaction
436 caused overpressure of Paleocene Dongying Formation in northwest Liaodongwan
437 Depression, Bohai Bay Basin, China. *Journal of Petroleum Science and Engineering*,
438 147: 726-734. <http://dx.doi.org/10.1016/j.petrol.2016.09.014>
- 439 Wilkinson, M., Haszeldene, Haszeldene, R. S., and Fallick, A. E., 2006. Hydrocarbon filling
440 and leakage history of a deep geopressed sandstone, Fulmar Formation, United
441 Kingdom North Sea. *AAPG Bulletin*, 90: 1945-1961.
442 <http://dx.doi.org/10.1306/06270605178>
- 443 Xu, C., Jiang, P., Wu, F., Yang, B., and Li, D., 2002. Discovery and sedimentary
444 characteristics of the Neogene delta in Bozhong depression and its significance for oil
445 and gas exploration. *Acta Sedimentologica Sinica*, 20: 588-594. (in Chinese)
- 446 Xu, Z., Chen, S., and Wang, Y., 2006. Mesozoic tectonic activities and sedimentation in the
447 Bohai Gulf area. *Chinese Geology*, 33: 201-211. (in Chinese)
- 448 Yardley, G. S., and Swarbrick, R. E., 2000. Lateral transfer: A source of additional
449 overpressure. *Marine and Petroleum Geology*, 17: 523-538.
450 [http://dx.doi.org/10.1016/S0264-8172\(00\)00007-6](http://dx.doi.org/10.1016/S0264-8172(00)00007-6)
- 451 Zhou, X., Yu, Y., Tang, L., Lv, D., and Wang, Y., 2010. Cenozoic offshore basin architecture
452 and division of structural elements in Bohai sea. *China Offshore Oil and Gas (Geology)*,
453 22: 285-289. (in Chinese)
- 454 Zhu, W., Li, J., Zhou, X., and Guo, Y., 2008. Neogene shallow water deltaic system and large
455 hydrocarbon accumulations in Bohai Bay, China. *Acta Sedimentologica Sinica*, 26: 575-
456 582. (in Chinese)
- 457

458 **Figure captions**

459 Figure 1. Location and structural distribution of Bozhong Depression.

460 Figure 2. Summarized stratigraphic columns of offshore Bohai Bay Basin.

461 Figure 3. Burial and thermal history of Bozhong Depression.

462 Figure 4. Composition and grain size of the Es and Ed sandstones in Bozhong Depression.

463 Figure 5. Porosity versus depth in Bozhong Depression.

464 Figure 6. Porosity-permeability correlation in Bozhong Depression.

465 Figure 7. Measured data of pressure and temperature versus depth.

466 *The hydrostatic pressure gradient in this area is 10 MPa/km (0.442 psi/ft).

467 *Overlapped depth of different stratum is due to the difference of structural location.

468 Figure 8. Distribution maps and profiles of overpressure in Bozhong Depression.

469 Figure 9. The SEM images of Ed sandstones within different pore pressure horizons.

470 Figure 10. The SEM images of Es sandstones within different pore pressure horizons.

471 Figure 11. The relationship of porosity and vertical effective stress in Bozhong Depression.

472 Figure 12. The schematic diagram of the relationship between VES and porosity.